Journal of Thermal Analysis and Calorimetry (2020) 142:2341–2349
https://doi.org/10.1007/s10973-020-09269-8

Synthesis of a Valen Schiff-base bismuth(III) complex and its thermokinetic studies on the growth metabolism of *S. pombe*

Jian-Hong Jiang[1] · Xu Li[1] · Chuan-Hua Li[1] · Fan-Hua Zeng[1] · Zhao-Biao Mou[1] · Rou Zou[1] · Sha Qu[1] · Li-Juan Ye[1] · Qiang-Guo Li[1]

Received: 2 November 2019 / Accepted: 1 January 2020 / Published online: 21 January 2020

Abstract
A Valen Schiff-base ligand [1,5-bis(2-hydroxy-3-methoxybenzylidene)thiocarbonohydrazide] and its bismuth(III) complex were synthesized. The compositions and structures of two compounds were characterized by elemental analysis, spectrometry (^{1}HNMR, MS, FT-IR, and UV-visible), chemical analysis, molar conductivity, and TG–DTA analysis. The results showed that the molecular formula of Schiff base and its bismuth(III) complex was $C_{17}H_{18}O_4N_4S$ (abbreviated as H_2L, $L=C_{17}H_{16}O_4N_4S$) and $[Bi(C_{17}H_{16}O_4N_4S)Cl{\cdot}H_2O]$ (abbreviated as $[Bi(L)Cl{\cdot}H_2O]$), respectively. Furthermore, the thermokinetic properties of the action of Schiff base and its bismuth(III) complex on the growth metabolism of *S. pombe* were studied by bio-microcalorimetry at 305.15 K. The growth rate constant (k), maximum heat power, generation time, inhibition ratio (I) and half inhibition concentration (IC_{50}), and their quantitative relationship with the concentration were calculated, respectively. Experimental results indicated that both Schiff base and its bismuth(III) complex could inhibit the growth of *S. pombe*, but the inhibitory effect of Schiff base was stronger than that of the complex. The half inhibition concentrations of Schiff base and its bismuth(III) complex were found to be 4.17×10^{-3} mol L^{-1} and 6.13×10^{-3} mol L^{-1}, respectively.

Keywords *o*-Vanillin · Thiocarbonohydrazide · Bismuth(III) complex · *S. pombe* · Bio-microcalorimetry

Introduction

In recent years, the coordination chemistry has gained much attention owing to the synthesis and characterization of a large number of transition–metal complexes in which metal ion could be coordinated by oxygen, nitrogen, and sulfur [1]. Derived from the condensation reaction of primary amines and active carbonyl group, Schiff base possesses the azomethine group with a general formula $RHC=N–R_1$, where R and R_1 are substituted by different groups such as alkyl, aryl, and heterocyclic groups [2, 3]. Some studies have shown that the chemical and biological properties of Schiff base related to the presence of a lone pair of electrons in an sp^2 hybridized orbital of nitrogen atom of the azomethine group [4–6]. Thiosemicarbazones containing a thiourea moiety are an important class of Schiff bases in medicinal and pharmaceutical fields. Thiosemicarbazones and their metal complexes are well known for their biological activities such as anticancer [7, 8], antibacterial [9, 10], and antiparasitic activity [11, 12]. Research on the biological properties of thiosemicarbazones, as well as on those of their metal complexes, has been extensively investigated, while their bismuth(III) complexes are still less studied [1, 13]. One reason may be that because bismuth ion is easy to hydrolyze, the suitable single crystals are difficult to be obtained for the X-ray diffraction [14]. Due to their high effectiveness, low toxicity, and low radioactivity [15, 16], bismuth and its compounds have been applied in the treatment involving syphilis, diarrhea, gastritis, and colitis. In addition, bismuth compounds also possess anticancer activities [17].

S. pombe, also called "fission yeast," has become model organism for studying eukaryotic cells, playing an important role in revealing the mechanism of life activities [18]. Compared with mammalian cells, yeast cells are similar in

✉ Chuan-Hua Li
lichuanhua0526@126.com

✉ Qiang-Guo Li
liqiangguo@163.com

[1] Hunan Provincial Key Laboratory of Xiangnan Rare-Precious Metals Compounds and Applications, College of Chemical Biology and Environmental Engineering, Xiangnan University, Chenzhou 423043, Hunan Province, People's Republic of China

inheritance and evolution, but faster and easier to culture. A series of findings of human cells were firstly discovered by yeast cells [19]. Microcalorimetry, which is a general, non-destructive, and highly sensitive method based on biological thermokinetics, has been applied in monitoring biological metabolic activities of cells, and this way has some advantages over traditional methods like Oxford cup method and Agar dilution method [20–22].

In this study, as a part of our continuing studies [23–25], we report here the synthesis of a Valen Schiff base by the condensation of *o*-Vanillin and thiocarbohydrazide. The bismuth(III) complex was prepared reacting of Schiff base and $BiCl_3$. Newly synthesized complex with its corresponding ligand was characterized by means of physical and spectral analyses. They were also tested for their antibacterial activity against *S. pombe* by bio-microcalorimetry. Some thermokinetic parameters were obtained. The purpose of this paper is to provide some thermokinetic parameters for further study of bismuth compounds.

Experimental

Instrumentation and materials

o-Vanillin (≥ 99.0%); thiocarbonohydrazide (TCH, A.R.); $BiCl_3$ (A.R.); NaCl (A.R.); $AgNO_3$ (A.R.); EDTA (A.R.); methanol (A.R.); ethanol (A.R.); *N*, *N*-dimethylformamide (DMF, A.R.); dimethyl sulfoxide (DMSO, A.R.). All of above reagents were purchased from the Sinopharm Chemical Reagent Co., Ltd. (Shanghai, China) and used without any further purification.

S. pombe (ACCC 20047) was bought from Beijing Century Aoke Biological Technology Co., Ltd. YES medium: yeast (5.000 g), glucose (30.000 g), *L*-Leu (0.225 g), *L*-Lys (0.225 g), *L*-His (0.225 g), adenine (0.225 g), and uracil (0.225 g), which was dissolved in 1000 mL water. The medium was obtained after being autoclaved at 120 °C for 30 min.

^{1}H NMR spectrometer (Bruker 400 MHZ, Sweden); mass spectrometer (Thermofinnigan MAT 95 XP USA); elemental analyzer (Perkin-Elmer 240 CHNS, USA); FT-IR spectrometer (Avatar 360, with KBr pellets, USA); UV-Vis spectrometer (HITACHIU-3010, Japan); biological microcalorimeter (TAM air 3116-2/3239, Switzerland); conductometer (DDS-12DW, Shanghai, China); stereo micro melting point instrument (XT4, Beijing, China); and thermogravimetric and differential thermal analyzer (HCT-3, Beijing, China).

Synthesis of Schiff base

Twelve mmol *o*-vanillin was dissolved in 60 mL ethanol, and 6 mmol thiocarbonohydrazide was dissolved in 60 mL water. Then, the solution of thiocarbonohydrazide was slowly added dropwise into the ethanol solution of *o*-vanillin and the mixture was stirred on a water bath at 60 °C for 5 h. As the reaction progressed, the color of the solution became yellow-green. After cooling to room temperature and standing for 12 h, the yellow-green precipitate was collected and washed with ethanol and water at 60 °C alternately, then dried in a vacuum desiccator. Finally, the yellow-green powder of Schiff base was obtained with a yield of 78.1%. The theoretical values for the elemental analysis of Schiff base are as follows: C, 54.53%; H, 4.85%; N, 14.96%; and S, 8.56%. The found values are as follows: C, 54.51%; H, 4.80%; N, 15.02%; and S, 8.58%. The ^{1}H NMR (400 MHz, DMSO-d_6) data are as follows: 12.09 (*d*, 2H, OH), 11.61 (*s*, 1H, NH), 9.33 (*s*, 1H, NH), 8.57 (*t*, 2H, CH=N), 7.94-6.59 (m, 6H, Ar–H), 3.83 (*s*, 6H, OCH_3), and ESI–MS (*m*/*z*): 374.8 (M^+) (Calcd. $M = 374.4$).

Synthesis of the complex

A 2.8 mmol Schiff base was dissolved in 80 mL acetone. A 2.8 mmol $BiCl_3$ was dissolved in 20 mL THF, and a clear solution was obtained. This clear THF solution of $BiCl_3$ was added dropwise into the acetone solution of Schiff base. The mixture was stirred at room temperature for 5 h. After standing for 12 h, the brown precipitate was collected and washed. The brown powder of the complex was obtained with a yield of 58.9%. The chemical composition of the complex was determined by elemental analysis for C, H, N, and S, by EDTA titration for Bi^{3+} and $AgNO_3$ titration for Cl^-. The theoretical values for the elemental analysis of the complex are as follows: C, 32.16%; H, 2.82%; N, 8.83%; S, 5.05%; Bi, 32.92%; Cl, 5.58%. The found values are: C, 32.15%; H, 2.80%; N, 8.84%; S, 5.09%; Bi, 32.84%; and Cl, 5.52%. The ^{1}H NMR (400 MHz, DMSO-d_6) data are as follows: 11.92–10.81 (*m*, 2H, NH), 8.48–7.87 (*m*, 2H, CH=N), 7.48–6.21 (*m*, 6H, Ar–H), and 4.22–3.51 (m, 6H, OCH_3).

Thermokinetic studies on growth metabolism of *S. pombe* treated by Schiff base and its complex

The thermokinetic studies on growth metabolism of *S. pombe* treated by Schiff base and its complex were carried out on a TAM Air microcalorimeter at 305.15 K. The details about the principle and structure of the instrument were given in literature [25]. When the system obtained a stable baseline, 5 mL of YES media and equal account of *S. pombe* were added into 8 ampoules. Then, Schiff base and its complex at increased concentrations were added into the ampoules, respectively. All the ampoules were shaken, numbered, covered with caps, and pressed with special pliers. The ampoules in turn were hanged into the 8-channel

calorimeter block, and the thermokinetic curves were recorded until the recorder returned to the baseline.

Results and discussion

Characterization

General properties of Schiff base and its complex

Schiff base was obtained as a yellow-green powder. It could be dissolved in DMF, DMSO, acetone, ethanol, and THF and was soluble slightly in methanol but insoluble in water and petroleum ether. The molar conductivity of Schiff base (0.001 mol L^{-1}) in DMSO was determined to be 2.11 S cm^2 mol^{-1} at 298.15 K, which indicates that Schiff base was a nonelectrolyte. The melting point of Schiff base was determined to be 225 ± 1 °C by using binocular stereo micro melting point instrument.

The complex was obtained as a brown powder, which could be dissolved in DMF and DMSO and was soluble slightly in acetone and ethanol but insoluble in water, methanol, and petroleum ether. The molar conductivity of the complex (0.001 mol L^{-1}) in DMSO was determined to be 36.3 S cm^2 mol^{-1} at 298.15 K, which means that the complex was a nonelectrolyte. The melting point of complex was determined to be 252 ± 1 °C by using binocular stereo micro melting point instrument.

IR spectra and UV spectra of Schiff base and its complex

As shown in Fig. 1, a very sharp absorption of Schiff base at 1619 cm^{-1} was observed due to C=N and the absorption of *o*-Vanillin at 1640 cm^{-1} was vanished, indicating that Schiff base was synthesized. The absorption of C=N of the complex at 1602 cm^{-1} means that C=N took part in coordination. In addition, the absorption of Ph-O at 1252 cm^{-1} red-shifted to 1246 cm^{-1} compared with Schiff base, indicating that Ph–O was coordinated. The peak near 1058 cm^{-1} is assigned to υ(C=S) stretching of the thione C=S group [26]. Upon coordination, the absence of the peak at 1058 cm^{-1}(C=S) combined to the appearance of a peak near 731 cm^{-1}(C−S) indicates evidence for the coordination of the sulfur to the metal center. In low wavelength range, new absorptions at 552 cm^{-1} and 446 cm^{-1} appeared, corresponding to Bi–O and Bi–N, respectively, confirming that N and O atoms were coordinated with Bi^{3+}. The broad absorption at 3520 cm^{-1} is due to OH, which means the complex contains water.

The UV spectrum of DMSO solution (0.0010 mol L^{-1}) of *o*-vanillin, thiocarbonohydrazide, Schiff base, and its complex was measured. The details of UV spectra were shown in Fig. 2. As we can see, there were remarkable differences between the UV spectrum of these samples. As for Schiff base, a weak absorption at 242 nm was due to π–π* transition of the phenyl rings, and a wide and strong absorption at 321–363 nm belongs to the π–π* and n–π* transition of C=N. There was a strong absorption at 245 nm after the complex formed. The absorption at 321–368 nm of the complex had an evident red-shift owing to the number of phenyl rings of the complex and the larger delocalization conjugate systems were formed. Moreover, the absorption of the complex at 439 nm, indicating that Schiff base, was coordinated with Bi^{3+}.

Mechanism of thermal decomposition

TG–DTA curves of the complex at a heating rate of 10 °C/min in a static air atmosphere from room temperature to 850 °C were shown in Table 1. The thermal decomposition

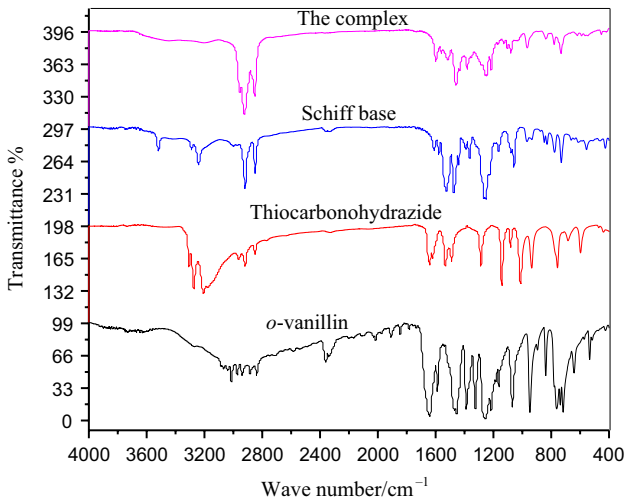

Fig. 1 IR spectra of *o*-vanillin, thiocarbonohydrazide, Schiff base, and its complex

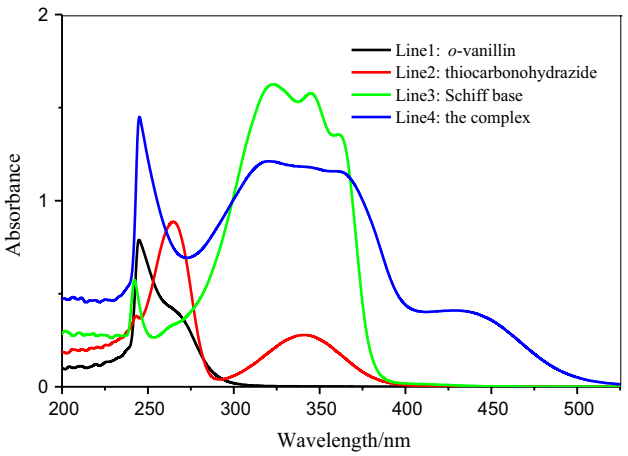

Fig. 2 UV spectra of *o*-vanillin, thiocarbonohydrazide, Schiff base, and its complex. (Color figure online)

Table 1 TG-DTA data of bismuth(III) complex [Bi($C_{17}H_{16}O_4N_4S$) Cl·H_2O]

	Temperature range/°C	Mass loss Calc(found)%	Decomposition group	Remainder
First step	218–257	8.43 (8.46)	H_2O, Cl	Bi($C_{17}H_{16}O_4N_4S$)
Second step	257–412	17.9 (17.4)	CH_4N_4S	Bi($C_{16}H_{12}O_4$)
Third step	412–545	51.15 (51.13)	$C_{16}H_{12}O_4$	Bi_2O_3

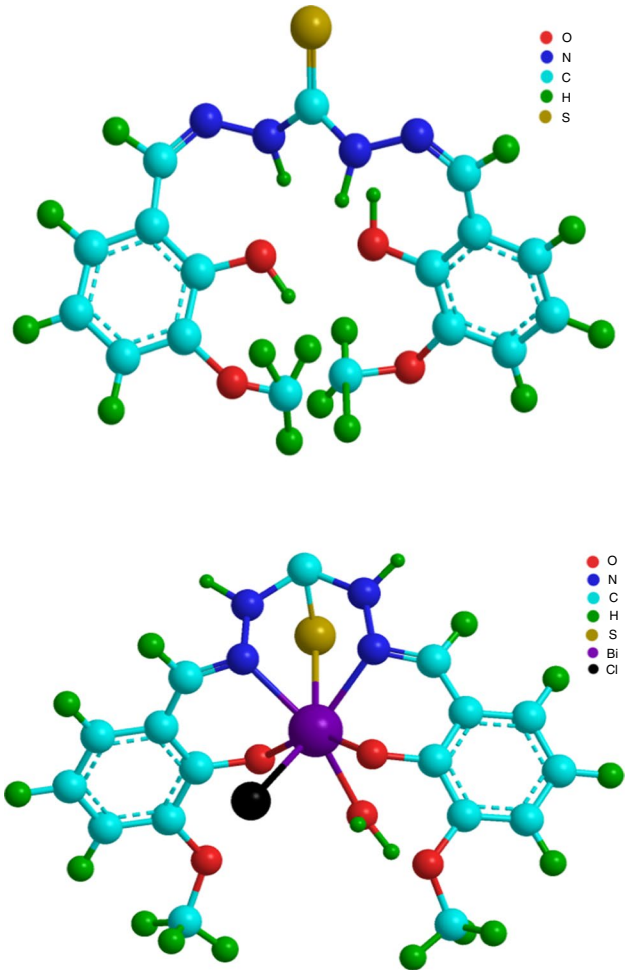

Fig. 3 Chemical structures of Schiff base (**a**) and its complex (**b**). (Color figure online)

process can be divided into three steps. The first process, it had a weak endothermic peak ranging from 218 to 257 °C with a mass loss of 8.46%, which was close to the theoretical value (8.43%) due to the loss of 1 mol H_2O and Cl. The second process, it had a strong endothermic peak, ranging from 257 to 412 °C with a mass loss of 17.4%, which corresponds to the loss of 1 mol of CH_4N_4S from the complex (theoretical value is 17.9%). In the last step, it had a strong endothermic peak, corresponding to the temperature range from 412 to 545 °C with a mass loss of 51.13%, which was similar to the theoretical value (51.15%) roughly. The complex was decomposed into Bi_2O_3, which meant all of the ligands were lost. On the basic of the experimental and calculated results, the molecular formula of the complex is [Bi($C_{17}H_{16}O_4N_4S$) Cl·H_2O], whose thermal decomposition is as follows:

$$2[Bi(C_{17}H_{16}O_4N_4S)]Cl \cdot H_2O \xrightarrow{218-257\,^{\circ}C} 2[Bi(C_{17}H_{16}O_4N_4S)] \xrightarrow{257-412\,^{\circ}C} 2[Bi(C_{16}H_{12}O_4)] \xrightarrow{412-545\,^{\circ}C} Bi_2O_3$$

In sum, it was inferred that the molecular formula of Schiff base and its complex was $C_{17}H_{18}O_4N_4S$ and [Bi($C_{17}H_{16}O_4N_4S$) Cl·H_2O], respectively. Their possible chemical structures were given in Fig. 3.

Determination of thermokinetic parameters of Schiff base and its complex on *S. pombe* growth

Power–time curves for the growth of *S. pombe*

Through the ampoule method, the power–time curves for the growth of *S. pombe* treated by different concentrations of Schiff base and its complex were recorded at 305.15 K, respectively. The thermogenic curves were shown in Figs. 4 and 5. As can be seen in Figs. 4 and 5, with the increase of concentrations of the drugs, the heat production for the growth of *S. pombe* decreased, and the maximum heat output (P_{max}) could be obtained easily. The P_{max} values were listed in Table 2.

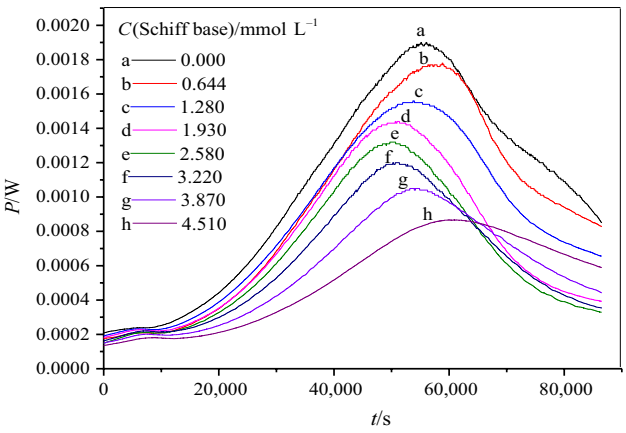

Fig. 4 Power–time curves of the growth of *S. pombe* affected by Schiff base

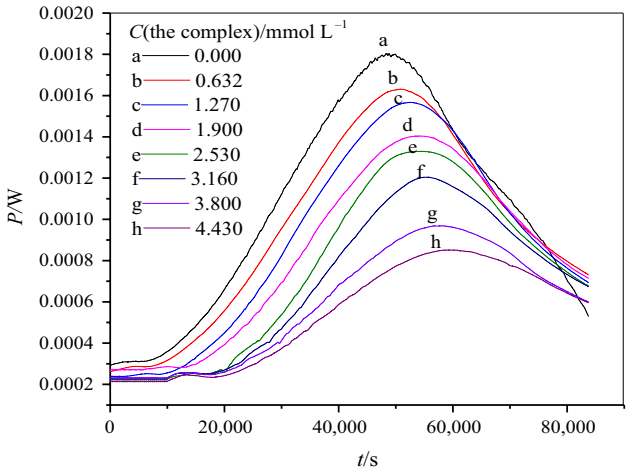

Fig. 5 Power–time curves of the growth of *S. pombe* affected by the complex

The growth rate constant (*k*) and generation time (t_G) of *S. pombe*

The power–time curves of *S. pombe* could be divided into four phases, that is a lag phase, a log phase, a stationary phase, and a decline phase. During the log phase, the power–time curves obey the following equation [27]:

$$n_t = n_0 \exp[k(t-t_0)] \quad (1)$$

where $(t-t_0)$ is the period of time when t is the time after the start of exponential growth phase, and t_0 is the start time of exponential growth phase; n_t and n_0 are the cell number at time t and t_0, and k is the growth rate constant whose size represents growth speed. If the power output of each cell is w, then

$$n_t w = w n_0 \exp[k(t-t_0)] \quad (2)$$

If $P_t = n_t w$, $P_0 = n_0 w$, then

$$P_t = P_0 \exp[k(t-t_0)] \quad (3)$$

then

$$\ln P_t = \ln P_0 + kt - kt_0 \quad (4)$$

After doing the logarithmic treatment of P by using the Origin, we can obtain ln$P$–t curves at different concentrations. And then fitting ln$P$ and t were in linear increasing section to a line equation, the slopes were the growth rate constant (k). In addition, the generation time (t_G) whose size represents division and reproduction of *S. pombe* directly. The function relationship between k and t_G was shown as follows:

$$t_G = \ln 2/k \quad (5)$$

Table 2 Thermokinetic parameters of the growth of *S. pombe* affected by different concentrations of Schiff base and its complex at 305.15 K

Drugs	C^a/mol L^{-1}	k^b/s^{-1}	R	I^c/%	IC_{50}^d/mol L^{-1}	P_{max}/W	t_G/s
Schiff base	0	5.2555×10^{-5e}	0.9963	0	4.17×10^{-3}	1.9643×10^{-3}	1.3189×10^{4}
	6.44×10^{-4}	5.0506×10^{-5}	0.9904	3.90		1.4108×10^{-3}	1.3724×10^{4}
	1.28×10^{-3}	5.0033×10^{-5}	0.9937	4.80		1.2573×10^{-3}	1.3854×10^{4}
	1.93×10^{-3}	4.4696×10^{-5}	0.9844	14.95		9.7713×10^{-4}	1.5508×10^{4}
	2.58×10^{-3}	3.9097×10^{-5}	0.9876	25.61		6.6242×10^{-4}	1.7729×10^{4}
	3.22×10^{-3}	3.8825×10^{-5}	0.9949	26.13		5.3301×10^{-4}	1.7854×10^{4}
	3.87×10^{-3}	3.2920×10^{-5}	0.9927	37.36		3.8343×10^{-4}	2.1056×10^{4}
	4.51×10^{-3}	1.8947×10^{-5}	0.9904	63.90		2.4779×10^{-4}	3.6584×10^{4}
The complex	0	5.4415×10^{-5}	0.9973	0	6.13×10^{-3}	1.8038×10^{-3}	1.2738×10^{4}
	6.32×10^{-4}	4.8436×10^{-5}	0.9937	10.99		1.6312×10^{-3}	1.4311×10^{4}
	1.27×10^{-3}	4.7120×10^{-5}	0.9844	13.41		1.5674×10^{-3}	1.4710×10^{4}
	1.90×10^{-3}	4.6513×10^{-5}	0.9903	14.52		1.4042×10^{-3}	1.4902×10^{4}
	2.53×10^{-3}	4.5239×10^{-5}	0.9899	16.86		1.3300×10^{-3}	1.5322×10^{4}
	3.16×10^{-3}	4.4992×10^{-5}	0.9846	17.32		1.2044×10^{-3}	1.5406×10^{4}
	3.80×10^{-3}	4.0816×10^{-5}	0.9909	24.99		9.6876×10^{-4}	1.6982×10^{4}
	4.43×10^{-3}	3.7482×10^{-5}	0.9904	31.17		8.5176×10^{-4}	1.8493×10^{4}

[a]The concentration

[b]The growth rate constant of *S. pombe*

[c]The inhibition ratio

[d]The half inhibition concentration

[e]Mean ± S.D.; $n=3$

The t_G of *S. pombe* were calculated at different concentrations of Schiff base and its complex, as summarized in Table 2.

The inhibition ratio (*I*) of *S. pombe*

The inhibition ratio (I) represents the inhibition degree of cells at different concentrations of drugs. In order to study the effect of Schiff base and its complex on the growth of *S. pombe*, defining the inhibition as:

$$I = \frac{(k_0 - k_c)}{k_0} \times 100\% \tag{6}$$

where k_0 is the growth rate constant without any drugs of *S. pombe,* and k_c is the constant of *S. pombe* treated by the drugs at concentration of c. The values of I were also shown in Table 2. IC_{50} means that when the inhibition ratio is 50%, the drug concentration is the half inhibition concentration.

Quantitative relationship between thermokinetic parameters and concentrations of Schiff base and its complex

Quantitative relationship between *k* and *C*

As can be seen in Table 2, with the increase of the concentration of the drugs, the growth rate constant (k) of *S. pombe* decreased, which means that both Schiff base and its complex have inhibition effects on the growth of *S. pombe*. Plotting the inhibition ratio (k) against the concentration (c) of Schiff base and its complex, Fig. 6 was produced. The curve equations were obtained by using the logistic curve fitting from data of the growth rate constant (k) of *S. pombe* with concentration (c) of Schiff base and its complex (as shown in Eq. (7) and (8)), in which the correlation coefficients R of Schiff base and its complex were 0.9912 and 0.9208, respectively.

$$k = -11957.63 + \frac{11962.69}{1 + \left(\frac{c}{192.65}\right)^{2.22}}$$
$$(0.00\,\text{mol}\,\text{L}^{-1} \le C_{\text{Schiff base}} \le 4.51 \times 10^{-3}\text{mol}\,\text{L}^{-1}) \tag{7}$$

$$k = -5600.57 + \frac{5605.84}{1 + \left(\frac{c}{322673.47}\right)^{0.75}}$$
$$(0.00\ \text{mol}\,\text{L}^{-1} \le C_{\text{the complex}} \le 4.43 \times 10^{-3}\ \text{mol}\,\text{L}^{-1}) \tag{8}$$

Quantitative relationship between *I* and *C*

The *I–C* curves were made relied on the inhibition ratio (I) and the different concentrations of Schiff base and its complex. As shown in Fig. 7, in low-concentration levels, with the increase of the concentrations of the drugs, the inhibition ratio (I) of *S. pombe* increased, and in high-concentration levels, the slopes of curves increased rapidly that means drugs have strong inhibition effects on *S. pombe*. Within the scope of the studied concentrations, carries on the curves fitting to inhibition rate I and the concentration c, and the curve equations were given in Eqs. (9) and (10). The corresponding correlation coefficients R of Schiff base and its complex were 0.9295 and 0.9202, respectively.

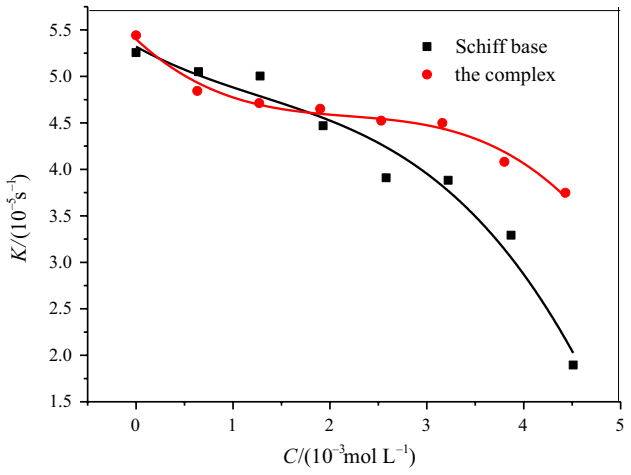

Fig. 6 Relationships between the growth rate constant (k) of *S. pombe* and the concentrations of Schiff base and its complex

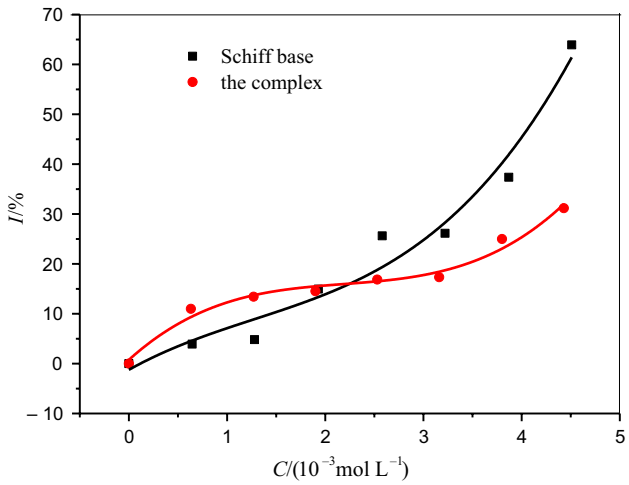

Fig. 7 Relationships between the inhibition ratio (I) of *S. pombe* and the concentrations of Schiff base and its complex

$$I = 495156.54 - \frac{495154.16}{1 + \left(\frac{c}{308.49}\right)^{2.15}}$$
$$(0.00\ \text{mol}\,\text{L}^{-1} \le C_{\text{Schiff base}} \le 4.51 \times 10^{-3}\ \text{mol}\,\text{L}^{-1}) \quad (9)$$

$$I = 117572.59 - \frac{117569.46}{1 + \left(\frac{c}{365756.45}\right)^{0.75}}$$
$$(0.00\ \text{mol}\,\text{L}^{-1} \le C_{\text{the complex}} \le 4.43 \times 10^{-3}\ \text{mol}\,\text{L}^{-1}) \quad (10)$$

Quantitative relationship between P_{max} and C

Drawing the maximum heat output (P_{max}) of *S. pombe* growth against concentration(c), the curves were illustrated in Fig. 8. As shown in Fig. 8, with the increase of the concentrations of the drugs, the maximum heat output (P_{max}) of *S. pombe* decreased, and the curve equations were shown in Eqs. (11) and (12) by using the method of logistic, and the correlation coefficients R of Schiff base and its complex were 0.9917 and 0.9938, respectively.

$$P_{max} = -10.47 + \frac{12.43}{1 + \left(\frac{c}{60.47}\right)^{0.71}}$$
$$(0.00\ \text{mol}\,\text{L}^{-1} \le C_{\text{Schiff base}} \le 4.51 \times 10^{-3}\ \text{mol}\,\text{L}^{-1}) \quad (11)$$

$$P_{max} = -24483.39 + \frac{24485.17}{1 + \left(\frac{c}{28833.39}\right)^{1.16}}$$
$$(0.00\ \text{mol}\,\text{L}^{-1} \le C_{\text{the complex}} \le 4.43 \times 10^{-3}\ \text{mol}\,\text{L}^{-1}) \quad (12)$$

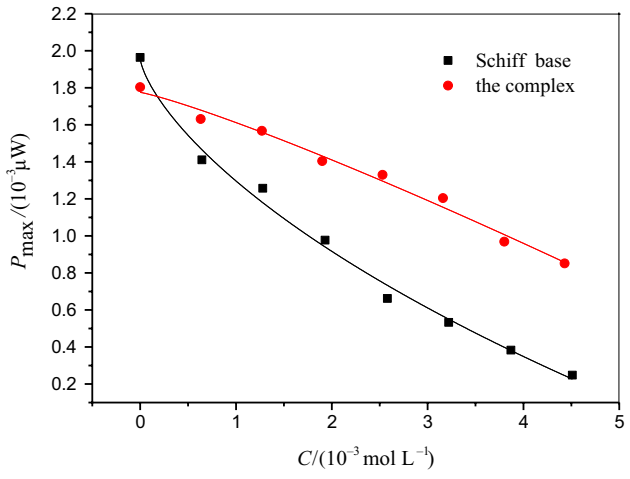

Fig. 8 Relationships between the maximum heat output (P_{max}) of *S. pombe* and the concentrations of Schiff base and its complex

Quantitative relationship between t_G and C

According to Eq. (5), the generation time (t_G) varies inversely with the growth rate constant (k). The t_G–C curves could be made according to the generation time (t_G) and different concentrations of Schiff base and its complex. From Fig. 9, it can be seen that, in low-concentration levels, with the increase of drug concentrations, the generation time (t_G) of *S. pombe* was increased, in which there were similar behaviors in the high-concentration levels. However, in high-concentration levels, the slopes of the curve of Schiff base changed much fast than that of the complex. Using the logistic curve fitting from data of the generation time (t_G) of *S. pombe* with concentration (c) of Schiff base and its complex, the curve equations were produced (as shown in Eqs. 13, 14), and the correlation coefficients R of Schiff base and its complex were 0.9923 and 0.9527, respectively.

$$t_G = 8.36 - \frac{6.89}{1 + \left(\frac{c}{5.17}\right)^{6.32}}$$
$$(0.00\ \text{mol}\,\text{L}^{-1} \le C_{\text{Schiff base}} \le 4.51 \times 10^{-3}\text{mol}\,\text{L}^{-1}) \quad (13)$$

$$t_G = 5388.03 - \frac{5386.64}{1 + \left(\frac{c}{990.30}\right)^{1.76}}$$
$$(0.00\ \text{mol}\,\text{L}^{-1} \le C_{\text{the complex}} \le 4.43 \times 10^{-3}\text{mol}\,\text{L}^{-1}) \quad (14)$$

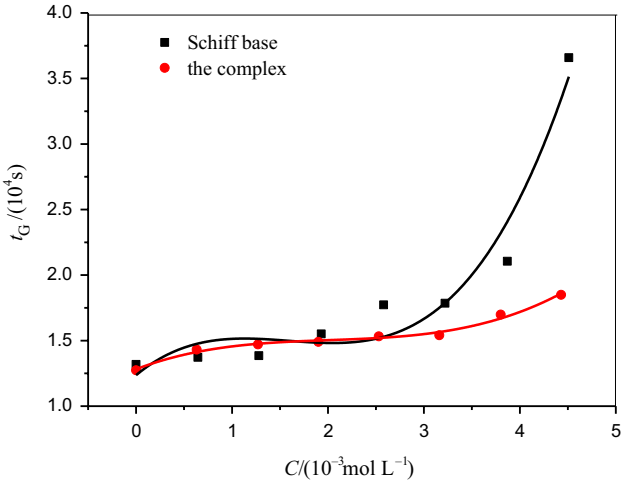

Fig. 9 Relationships between the generation time (t_G) of *S. pombe* and the concentrations of Schiff base and its complex

Conclusions

The work described in this paper was the synthesis and characterization of a Valen Schiff base and its bismuth(III) complex. Their compositions and structures were characterized by using different physiochemical techniques. Moreover, the thermokinetics of Schiff base and its bismuth(III) complex on growth metabolism of *S. pombe* were studied, finding that both two compounds had inhibition effects on *S. pombe* cells, and the inhibition effects were increased with the increase of concentrations. Some thermokinetic parameters (k, P_{max}, t_G, and I) and their quantitative relationship with concentration were investigated.

Acknowledgements The authors thank the National Natural Science Foundation of China (No. 21273190), The Hunan Provincial Natural Science Foundation of China (No. 2017JJ2240), The Project of Scientific Research of Hunan Provincial Education Department (18B499, 15A175, 14A134, 15C1272, and 16C1492, 17C1472), Science and Technology Plan Projects of Hunan Province (2014FJ3011, 2011TP4016-1, and 2012TP4021-5), the National Students' Project for Innovation and Entrepreneurship Training Program (No.201910545038), and Science and Technology Plan Project of Chenzhou city (CKJ2016020) for financial support.

References

1. Arion VB. Coordination chemistry of S-substituted isothiosemicarbazides and isothio- semicarbazones. Coord Chem Rev. 2019;387:348–97.
2. Belal AAM, El-Deen IM, Farid NY, Zakaria R, Refat MS. Synthesis, spectroscopic, coordination and biological activities of some transition metal complexes containing ONO tridentate Schiff base ligand. Spectrochim Acta A. 2015;149:771–87.
3. Liu X, Hamon JR. Recent developments in penta-, hexa- and heptadentate Schiff base ligands and their metal complexes. Coord Chem Rev. 2019;389:94–118.
4. More P, Bhalvankar RB, Pattar SC. Synthesis and biological activities of Schiff bases of aminothiazoles. J Indian Chem Soc. 2001;78:474–5.
5. Kabak M, Elmali A, Elerman Y. Keto-enol tautomerism, conformations and structure of *N*-(2-hydroxy-5-methylphenyl), 2-hydroxybenzaldehydeimine. J Mol Struct. 1999;477:151–8.
6. Spichiger-Keller U. Chemical sesors and biosensors for medical and biological applications. Weinheim: Wiley; 1998. ISBN 3-527-28855-4.
7. Zaltariov MF, Hammerstad M, Arabshahi HJ, Jovanovic K, Richter KW, Cazacu M, Shova S, Balan M, Andersen NH, Radulovic S, Reynisson J, Andersson KK, Arion VB. New iminodiacetate–thiosemicarbazone hybrids and their copper(II) complexes are potential ribonucleotide reductase R2 inhibitors with high antiproliferative activity. Inorg Chem. 2017;56:3532–49.
8. Stacy AE, Palanimuthu D, Bernhardt PV, Kalinowski DS, Jansson PJ, Richardson DR. Zinc(II)-thiosemicarbazone complexes are localized to the lysosomal compartment where they transmetallate with copper ions to induce cytotoxicity. J Med Chem. 2016;59:4965–84.
9. Netalkar PP, Netalkar SP, Netalkar VK. Transition metal complexes of thiosemicarbazone: synthesis, structures and invitro antimicrobial studies. Polyhedron. 2015;100:215–22.
10. Oliveira AA, Perdigao GMC, Rodrigues LE, Silva JG, Souza-Fagundes EM, Takahashi JA, Rocha WR, Beraldo H. Cytotoxic and antimicrobial effects of indium(III) complexes with 2-acetylpyridine-derived thiosemicarbazones. Dalton Trans. 2017;46:918–32.
11. Chellan P, Land KM, Shokar A, Au A, An SH, Clavel CM, Dyson PJ, Kock C, Smith PJ, Chibale K, Smith GS. Exploring the versatility of cycloplatinated thiosemicarbazones as antitumor and antiparasitic agents. Organometallics. 2012;31:5971–9.
12. Adams M, Kock C, Smith PJ, Land KM, Liu N, Hopper M, Hsiao A, Burgoyne AR, Stringer T, Meyer M, Wiesner L, Chibalea K, Smith GS. Improved antiparasitic activity by incorporation of organosilane entities into half-sandwich ruthenium(II) and rhodium(III) thiosemicarbazone complexes. Dalton Trans. 2015;44:2456–68.
13. Casas JS, Garcia-Tasende MS, Sordo J. Main group metal complexes of semicarbazones and thiosemicarbazones. A structural review. Coord Chem Rev. 2000;209:197–261.
14. Li MX, Yang M, Niu JY, Zhang LZ, Xie SQ. A nine-coordinated bismuth(III) complex derived from pentadentate 2,6-diacetylpyridine bis(^{4}*N*-methylthiosemicarbazone): crystal structure and both in vitro and in vivo biological evaluation. Inorg Chem. 2012;51:12521–6.
15. Nomiya K, Sekino K, Ishikava M, Honda A, Yokoyama M, Kasuga NC, Yokoyama H, Nakano S, Onodera K. Syntheses, crystal structures and antimicrobial activities of monomeric 8-coordinate, and dimeric and monomeric 7-coordinate bismuth(III) complexes with tridentate and pentadentate thiosemicarbazones and pentadentate semicarbazone ligands. J Inorg Biochem. 2004;98:601–15.
16. Andrews PC, Ferrero RL, Forsyth CM, Junk PC, Maclellan JG, Peiris RM. Bismuth(III) saccharinate and thiosaccharinate complexes and the effect of ligand substitution on their activity against *Helicobacter*. Organometallics. 2011;30:6283–91.
17. Briand GG, Burford N. Bismuth compounds and preparations with biological or medicinal relevance. Chem Rev. 1999;99:2601–57.
18. Cortes JC, Carnero E, Ishiguro J, Sanchez Y, Durán A, Ribas JC. The novel fission yeast (1,3)beta-D-glucan synthase catalytic subunit Bgs4p is essential during both cytokinesis and polarized growth. J Cell Sci. 2005;118:157–74.
19. Drgonova J, Drgon T, Tanaka K, Kollar R, Chen GC, Ford RA, Chan CSM, Takai Y, Cabib E. Rho1p, a yeast protein at the interface between cell polarization and morphogenesis. Science. 1996;272:277–9.
20. Chen C, Qu F, Wang J, Xia XH, Wang JB, Chen Z, Ma X, Wei SZ, Zhang YM, Li JY, Gong M, Wang RL, Liu HH, Yang ZR, Li YG, Zhao YL, Xiao XH. Antibacterial effect of different extracts from *Wikstroemia indica* on *Escherichia coli* based on microcalorimetry coupled with agar dilution method. J Therm Anal Calorim. 2016;123:1583–90.
21. Braissant O, Bachmann A, Bonkat G. Microcalorimetric assays for measuring cell growth and metabolic activity: methodology and applications. Methods. 2015;76:27–34.
22. Kong WJ, Zhao YL, Xing XY, Ma XP, Sun XJ, Yang MH, Xiao XH. Antibacterial evaluation of flavonoid compounds against *E. coli* by microcalorimetry and chemometrics. Appl Microbiol Biotechnol. 2015;99:6049–58.
23. Li CH, Tao X, Jiang JH, Li X, Xiao SX, Tao LM, Zhou JF, Zhang H, Xie MA, Zhu Y, Xia Z, Tang SM, Yuan HM, Li QG. Synthesis, crystal structure and spectroscopic studies of bismuth(III) complex with 2-substituted benzimidazole ligands. Spectrochim Acta A. 2016;166:56–61.

24. Li CH, Jiang JH, Li X, Tao LM, Xiao SX, Gu HW, Zhang H, Jiang C, Xie JQ, Peng MN, Pan LL, Xia XM, Li QG. Synthesis, crystal structure and biological properties of a bismuth(III) Schiff-base complex. RSC Adv. 2015;5:94267–75.
25. Li X, Jiang JH, Chen QQ, Xiao SX, Li CH, Gu HW, Zhang H, Hu JL, Yao FH, Li QG. Synthesis of nordihydroguaiaretic acid derivatives and their bioactivities on *S. pombe* and *K*562 cell lines. Eur J Med Chem. 2013;62:605–13.
26. Schader B. Infrared and Raman spectroscopy-methods and applications. Weinheim: Wiley; 1995. ISBN 3-527-26446-9.
27. Xie CL, Tang HK, Song ZH, Qu SS, Liao YT, Liu HS. Microcalorimetric study of bacterial growth. Thermochim Acta. 1988;123:33–41.